

A micromechanical model for magnetorheological fluids under slow compression

José Antonio Ruiz-López¹ · Roque Hidalgo-Alvarez¹ · Juan de Vicente¹

Received: 15 August 2015 / Revised: 21 January 2016 / Accepted: 22 January 2016 / Published online: 5 February 2016
© Springer-Verlag Berlin Heidelberg 2016

Abstract We propose a micromechanical model for the behavior of dilute magnetorheological fluids under unidirectional slow-compression, constant-volume squeeze flow mode. In the linear magnetization regime, the model predicts a power law scaling of the normal stress with the particle volume fraction and magnetic field strength squared at low fields. The predictions are satisfactorily compared with experimental measurements for different particle loadings, sample volume, surface roughness, and initial gap distance.

Keywords Magnetorheology · Magnetorheological fluids · Elongational flow · Yield stress · Squeeze flow · Yielding

Introduction

Magnetorheological (MR) fluids are field-responsive colloids that typically exhibit a liquid-to-solid transition upon the application of a magnetic field. In current commercial applications, MR fluids are subjected to strongly demanding deformations. Among standard kinematics, simple shear is undoubtedly the most widely studied and better known. However, the understanding of the squeeze flow behavior of MR fluids is still incomplete in spite of recent advances during the last decade (de Vicente et al. 2011a, 2011b; Ruiz-López et al. 2012; Guo et al. 2013; Xu et al. 2014).

Currently, continuum media theories are claimed to successfully explain their normal force versus gap dependence in slow-compression, no-slip conditions, under constant volume operation (see Fig. 2 in Ruiz-López et al. 2012; Guo et al. 2013; Xu et al. 2014). These theories predict the appearance of a yield compressive stress and a power law relationship between F and $1 - \varepsilon$ with exponent -2.5 (e.g., see Eq. 9 in de Vicente et al. 2011b). Here, F stands for the normal force and $\varepsilon = 1 - \frac{h}{h_0}$ is the compressive strain, where h is the gap distance and $h_0 = h(t=0)$ is the initial gap. Up to now, deviations between experiments and continuum media theory are qualitatively explained in terms of a shear strengthening effect (Tang et al. 2000) and demonstrated via superposition rheology (de Vicente et al. 2011b) and optical microscopy (Ruiz-López et al. 2012).

In this manuscript, we follow a microscopic approach to develop a slender-body like micromechanical model for the squeeze flow behavior of MR fluids in slow compression. The model accounts for magnetostatic forces between the particles and predicts the appearance of a yield compressive stress (and normal force) that scales with particle volume fraction and magnetic field squared, at low fields, in the linear magnetization regime. Strictly speaking, the validity of this model is limited to infinitesimally small deformations ($\varepsilon \rightarrow 0$) and for dilute suspensions ($\phi \rightarrow 0$), where single-particle-width chains should exist and interchain interactions are safely neglected. However, in spite of the many simplifications in this model, we will demonstrate here that it works well for a wide range of deformations ($\varepsilon \in [0 - 0.7]$) and concentrations ($\phi \in [0.001 - 0.10]$), and that it is also capable to enlighten some experimental findings reported in the literature that remain currently unexplained. In particular, the model predicts a $\log F$ versus $\log(1 - \varepsilon)$ slope of -2 in much better agreement with experimental data at very low loadings where the shear

✉ Juan de Vicente
jvicente@ugr.es

¹ Biocolloid and Fluid Physics Group, Department of Applied Physics, Faculty of Sciences, University of Granada, C/ Fuentenueva s/n., 18071 Granada, Spain

strengthening effect is expected to be negligible ($\phi \lesssim 0.05$) (Ruiz-López et al. 2012). In the second part of the manuscript, we describe carefully designed experiments at low particle concentrations to validate the model. Apart from these, we also address the influence of sample volume, surface roughness, and initial gap distance in the squeeze flow behavior.

Theoretical model

We assume a collection of single-particle-width chains confined between two parallel plates separated by a distance h and approaching with a velocity v . We assume that the gap h between the plates is much larger than the diameter of the (monodisperse) particles σ : $h \gg \sigma$. Also, we assume that v is small enough so that particles, initially forming straight chains in the field direction, readjust their positions into a thicker column but they do not spread out from the aggregate.

The magnetic dipolar energy for two particles with identical magnetic moments \vec{m}_i and \vec{m}_j separated at a distance r_{ij} follows the expression:

$$U_{ij} = \frac{1}{4\pi\mu_0\mu_{cr}} \frac{\vec{m}_i \cdot \vec{m}_j - 3(\vec{m}_i \cdot \hat{r})(\vec{m}_j \cdot \hat{r})}{r_{ij}^3} \quad (1)$$

where $\vec{m}_i = \vec{m}_j = \vec{m} = 3\mu_0\mu_{cr}\beta_p V_p \vec{H}$. Here, μ_0 is the magnetic permeability of the vacuum, μ_{cr} is the relative permeability of the continuous medium, β_p is the so-called contrast factor of the particles, $\beta_p = (\mu_{pr} - \mu_{cr})/(\mu_{pr} + 2\mu_{cr})$, μ_{pr} is the magnetic permeability of the particles, V_p is the particle volume, \hat{r} is the unit vector along the center-to-center line, and \vec{H} is the magnetic field strength. In this work, the magnetic field strength is calculated using the local field theory, $\vec{H} = \vec{H}_{loc}$ (Martin and Anderson 1996). According to this, the local field in the center

of a particle, i , can be calculated as $\vec{H}_{loc,i} = \vec{H}_0 + \sum_{j \neq i}^{N_{pc}} \vec{H}_{m_j}$,

where \vec{H}_0 is the external magnetic field, N_{pc} is the number of particles per chain, and $\vec{H}_{m_j} = \frac{3(\vec{m}_j \cdot \hat{r})\hat{r} - \vec{m}_j}{4\pi\mu_0\mu_{cr}r_{ij}^3}$ is the magnetic field produced by the magnetic dipole, \vec{m}_j located at the center of the particle i . Assuming an infinite and straight (no defects) single-particle-width chain aligned in the field direction, the local field becomes $\vec{H}_{loc} = (1 - \beta_p \zeta(3)/2)^{-1} \vec{H}_0$, where ζ is the Riemann Zeta function. Obviously, as a result of the approximations performed, the local field calculation is strictly valid in the limit of infinite gaps. However, for the gap intervals explored in this work, deviations are below 5%. It is important to remark here that the use of local fields instead of external fields is crucial because the local field is about 50 to 100% higher than the external magnetic field.

The total energy of a chain U_c is obtained by the addition of the contributions from all the pairs of particles within a chain:

$$U_c = \sum_{i=1}^{N_{pc}-1} \sum_{j=i+1}^{N_{pc}} U_{ij} \quad (2)$$

Under the hypothesis that $\sigma/h \ll 1$, it is possible to extend the summations in Eq. 2 to the continuum and hence, the magnetic energy in a chain can be written as

$$U_c = \int \frac{1}{4\pi\mu_0\mu_{cr}} \frac{d\vec{m} \cdot d\vec{m}' - 3(d\vec{m} \cdot \hat{r})(d\vec{m}' \cdot \hat{r})}{|\vec{r} - \vec{r}'|^3} \quad (3)$$

with $d\vec{m} = 3\mu_0\mu_{cr}\beta_a \vec{H} dV$ and $d\vec{m}' = 3\mu_0\mu_{cr}\beta_a \vec{H} dV'$. β_a is now the contrast factor of the aggregate: $\beta_a = (\mu_a - \mu_{cr})/(\mu_a + 2\mu_{cr})$. The magnetic permeability of the aggregates μ_a is estimated in this work using a mean field theory (e.g., Bötcher equation):

$$\frac{\mu_a - \mu_{cr}}{3\mu_a} = \phi_a \frac{\mu_p - \mu_{cr}}{2\mu_a + \mu_p} \quad (4)$$

For simplicity, we suppose now that the aggregates have a cylindrical shape and that they are thin enough to suppose that $dV = \pi r_c^2 dz$ and $dV' = \pi r_c^2 dz'$ where r_c is the radius of the cylinder. We also assume that the magnetic field points in the z -direction so $\vec{H} = H\hat{z}$. Then, the magnetic energy of a chain is obtained as follows:

$$U_c = -\frac{9}{2} \pi r_c^4 \mu_0 \mu_{cr} \beta_a^2 H^2 \int \frac{dz dz'}{|z - z'|^3} \quad (5)$$

The limits of integration in Eq. 5 come from the limits of the summations in Eq. 2. Thus, the summation from 1 to $N_{pc} - 1$ is now the integral of z from $\sigma/2$ to $h - 3\sigma/2$ and the summation from $j = i + 1$ to N_{pc} is the integral from $z + \sigma$ to $h - \sigma/2$. Bearing in mind that $\sigma \ll h$, after some algebra, Eq. 5 can be written as

$$U_c = -\frac{9}{4} \pi r_c^4 \mu_0 \mu_{cr} \beta_a^2 H^2 \left(\frac{h}{\sigma^2} - \frac{3}{\sigma} + \frac{1}{h} \right) \quad (6)$$

Next, the total energy of the system U is estimated by multiplying the energy of a chain U_c times the number of chains N_c ; $U = N_c U_c$. Here, the total number of chains N_c is obtained from the particle volume fraction in the system $N_c = 6\phi V_0 / \pi \sigma^2 h_0$ and the radius of the chain r_c can be obtained as a function of the initial radius of the chain r_{c0} . Here, we assume that the initial radius of the chain is the radius of the particle $r_{c0} = \sigma/2$ and that the volume of the aggregate remains constant during the compression $\pi r_c^2 h = \pi r_{c0}^2 h_0$. As a result, the following relation is

obtained: $r_c^4 = \sigma^4 h_0^2 / 16h^2$. Therefore, substituting r_c , the total energy U can be written as

$$U = -\frac{27}{32} \phi V_0 \mu_0 \mu_{cr} \beta_a^2 H^2 \left(\frac{h_0}{h} - \frac{3\sigma h_0^2}{h^2} + \frac{\sigma^2 h_0^3}{h^3} \right) \quad (7)$$

Considering $\sigma \ll h_0$ and the definition of the compressive strain, $\varepsilon = (h_0 - h)/h_0$, we arrive to the final expression of the magnetostatic energy:

$$U = -\frac{27}{32} \phi V_0 \mu_0 \mu_{cr} \beta_a^2 H^2 \frac{1}{1 - \varepsilon} \quad (8)$$

It is worth to note that the definition used for the compressive strain is only strictly valid for small deformations. For larger strains, the Hencky strain must be used $\varepsilon_H = \ln \frac{h}{h_0}$ (Engmann et al. 2005). In the case of large strains, $1/(1 - \varepsilon)$ should be replaced by e^{ε_H} .

With this, the normal stress in the sample is obtained as the derivative of the energy density with the instantaneous gap (de Vicente et al. 2011b):

$$\begin{aligned} \tau_{zz} &= -\frac{1}{S} \frac{\partial U}{\partial h} = -\frac{1}{Sh_0} \frac{\partial U}{\partial \varepsilon} = -\frac{1}{V} \frac{h}{h_0} \frac{\partial U}{\partial \varepsilon} \\ &= -\frac{1}{V} (1 - \varepsilon) \frac{\partial U}{\partial \varepsilon} \end{aligned} \quad (9)$$

Finally, substituting Eq. 8 into Eq. 9 we get

$$\tau_{zz} = \frac{27}{32} \phi \mu_0 \mu_{cr} \beta_a^2 H^2 \frac{1}{1 - \varepsilon} \quad (10)$$

From Eq. 10, the yield compressive stress τ_{YC} can be calculated as the normal stress τ_{zz} in the limit of no deformation (i.e., $\varepsilon \rightarrow 0$): $\tau_{YC} \equiv \lim_{\varepsilon \rightarrow 0} \tau_{zz} = \frac{27}{32} \phi \mu_0 \mu_{cr} \beta_a^2 H^2$. As a result, the yield compressive stress shows a linear dependence on the particle concentration ϕ and a quadratic dependence on the magnetic field strength H at low fields. These predictions are similar to those obtained from other micromechanical models reported in literature for yield shear stresses (Martin and Anderson 1996; de Gans et al. 1999; de Vicente et al. 2004; Volkova et al. 2000).

The magnetic normal force F can be obtained as the normal stress τ_{zz} multiplied by the surface area of the sample. There are two possibilities for the calculation of the surface area. On the one hand, we can assume that the field-induced structures slip along the surfaces and move radially when compressing. On the other hand, we can assume that the structures remain connecting the plates and do not displace radially. In the former case, the surface area can be simply calculated as $S = V_0/h$. In the latter case, the aggregates do not slip over the plates, the particle volume fraction increases within the gap according to $\phi = \phi_0 / 1 - \varepsilon$, and the surface area is given by $S = V_0/h_0$.

Nevertheless, no matter the particular assumption employed, we arrive to the same final equation for the magnetic normal force acting on the plates:

$$F = \frac{27}{32} \phi \mu_0 \mu_{cr} \beta_a^2 H^2 \frac{V_0}{h_0} \frac{1}{(1 - \varepsilon)^2} \quad (11)$$

Strictly speaking, apart from magnetostatic forces, capillary forces F_{cap} do, a priori, contribute as well to the normal force under compression (e.g., Ewoldt et al. 2011). F_{cap} depends on the surface tension γ , the contact angle, θ and the gap separation h according to: $F_{cap} = -2\gamma \cos(\theta) V_0/h^2$. It is an adhesive force ($F_{cap} < 0$), and therefore, it tends to diminish the gap between the plates. As observed, it depends on $(1 - \varepsilon)^{-2}$, similar to the magnetostatic contribution (c.f. Eq. 11). As a result, capillary forces contribute shifting (vertically) the normal force curves. For large particle concentrations and magnetic fields, F_{cap} is clearly much smaller than F because $F \propto \phi H^2$. However, capillary forces can be important in the case of small loadings and small fields. In order to avoid complications coming from capillary forces, the normal force transducer will be reset after loading the sample in the geometry. With this, the effect of the capillary force can be safely neglected at least in the limit of validity of the model (i.e., at low compressive strains).

Similar to τ_{YC} , a yield normal force F_Y can also be defined starting from Eq. 11:

$$F_Y \equiv \lim_{\varepsilon \rightarrow 0} F = \frac{27}{32} \phi \mu_0 \mu_{cr} \beta_a^2 H^2 \frac{V_0}{h_0} = \tau_{YC} \frac{V_0}{h_0} \quad (12)$$

As observed from Eqs. 10–12 predictions of this model are linear with the volume fraction and quadratic with the external magnetic field strength at low fields. On the one hand, the linearity with the volume fraction comes from the assumed arrangement of particles in single-particle-width chains at the beginning of the compression. Infinite dilution is a necessary condition for this to occur. On the other hand, the quadratic dependence with the magnetic field strength is a consequence of the linear magnetization approximation employed in the calculation of the magnetic moments of the particles, and it is strictly valid in the limit of low fields. Of course, a constant dependence with the field strength is expected in the saturation regime by simply replacing $\beta_a^2 H^2$ by $M_{as}^2/9$ (with M_{as} the saturation magnetization of the aggregates).

Experimental

Conventional MR fluids were prepared by carefully mixing carbonyl iron microparticles (HQ grade, BASF) in silicone oil of 20 mPa·s (Sigma-Aldrich). A parallel plate magnetorheometer MCR-501/MRD180 (Anton Paar) was used to perform constant volume squeeze flow experiments

in the presence of magnetic fields similarly to Ruiz-López et al. 2012. Details on the experimental setup can be found in Laun et al. (2008). Nonmagnetic titanium plates (diameter 20 mm) were employed except for the most concentrated MR fluids. Unless otherwise stated, the initial separation was $h_0 = 300 \mu\text{m}$ and the sample volume was $V_0 = 20 \mu\text{L}$. Plates were supposed to be perfectly parallel even though a small misalignment exists (Andablo-Reyes et al. 2010, 2011). Also, the distortion of the force sensor under pressures generated in this work and wall slip were neglected (de Vicente et al. 2011b). Wall slip was only noticeable for the highest concentrations and prevented using sandblasted plates. Magnetic fields were not too large (smaller than $\approx 300 \text{ kA/m}$) to minimize magnetic field gradients within the magneto cell (Laun et al. 2008).

All compression experiments reported here were run at constant volume V_0 , and constant velocity $v = 10 \mu\text{m/s}$ (elongational rate range: $\dot{\epsilon} \sim 0.03 - 0.2/\text{s}$). This corresponds to low plasticity numbers $S < 0.5$ and low Reynolds numbers $Re \sim 10^{-3} \ll 1$ so lubrication and creeping flow approximations can be used in the so-called filtration regime (McIntyre and Filisko 2010). The normal force sensor was zeroed after loading the sample in the geometry. Then, an external magnetic field was (suddenly) applied for 60 s for the field-induced structuration prior to the compression test. Results presented below are always averages over at least three separate runs. All experiments were run at $25 \text{ }^\circ\text{C}$.

Results and discussion

In Fig. 1, the model is compared to experimental data, for different external magnetic field strengths (from $H_0 = 88$ to 354 kA/m), on MR fluids formulated at a particle concentration of $\phi = 0.05$. We employ this particular loading as a reference (it is the same as in de Vicente et al. 2011b). Experimental data are represented as symbols, and solid lines correspond to theoretical predictions (Eq. 11). In this representation, experiments exhibit a slope of -2 in good agreement with the model. However, some deviations occur for the larger gap separations that could be due to inertia at the start-up of the compression test. Overall, a reasonably good quantitative agreement is found, bearing in mind that the model does not contain any free fitting parameter.

A more convenient way to visualize the experimental data is to plot a reduced force normalizing by the yield normal force, F_Y . From a theoretical point of view, this must result in a master scaling curve as a function of $1 - \epsilon$. Figure 2 represents theoretical and experimental data for a particle loading of $\phi = 0.05$. Generally speaking, a reasonably good scaling is found in agreement with the theory.

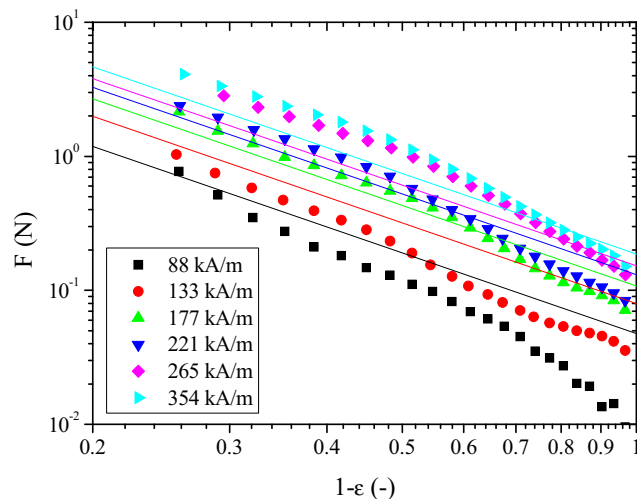


Fig. 1 Compression tests for $\phi = 0.05$ suspensions at different external magnetic field strengths. Symbols: experimental data. Lines: theoretical predictions (Eq. 11). Sample volume $V_0 = 20 \mu\text{L}$. Initial gap distance $h_0 = 300 \mu\text{m}$.

Effect of particle concentration

Next, we aim to explore the influence of particle concentration. From a theoretical perspective, it is expected a better agreement the lower the particle loading. Figure 3a demonstrates that the model satisfactorily explains the experimental data for low particle loadings. A very good agreement with the experiments is found for concentrations below $\phi = 0.10$. This was expected to be so because interactions between aggregates (*interaggregate* interactions) are not important for dilute systems and they are neglected in the theoretical model. Figure 3b demonstrates that the linear scaling with particle concentration predicted by the

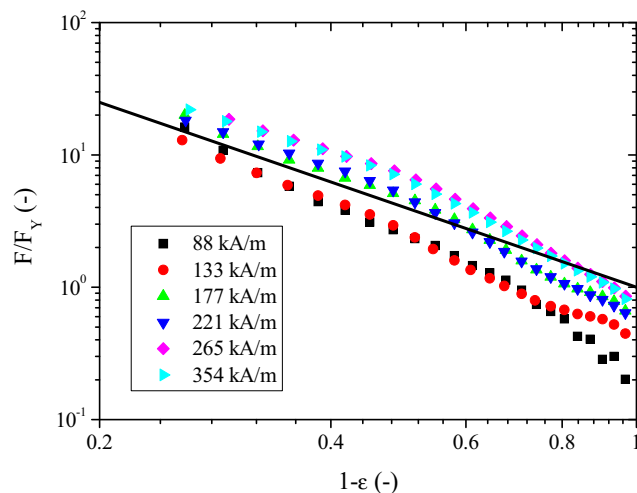
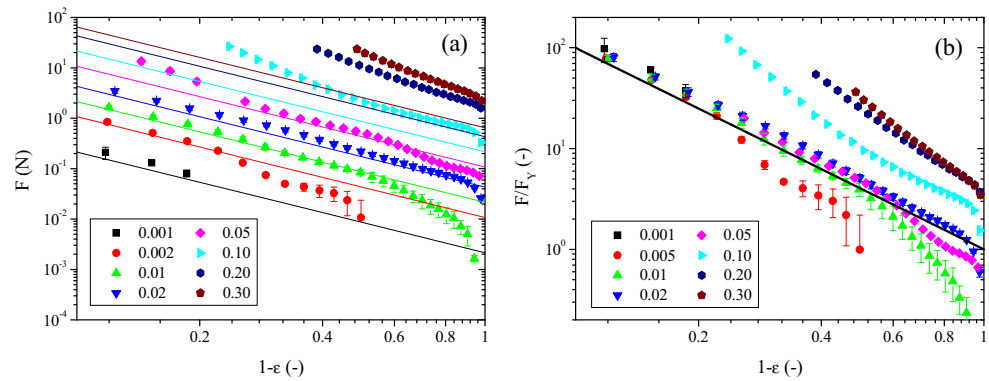


Fig. 2 Scaling compression curves for $\phi = 0.05$ suspensions at different external magnetic field strengths. Normal forces, F , are scaled here by the yield compressive stress $F_Y = \frac{27}{32} \phi \mu_0 \mu_{cr} \beta_a^2 H^2 \frac{V_0}{h_0}$. Symbols: experimental data. Line: theoretical prediction (Eq. 11). Sample volume $V_0 = 20 \mu\text{L}$. Initial gap distance $h_0 = 300 \mu\text{m}$.

Fig. 3 Effect of particle loading ϕ . *Symbols*: experimental data. *Lines*: theoretical predictions (Eq. 11). Sample volume $V_0=20\ \mu\text{L}$. Initial gap distance, $h_0=300\ \mu\text{m}$. Magnetic field strength, $H_0=177\ \text{kA/m}$. **a** Normal force, F , as a function of $1-\varepsilon$. **b** Normal force, F , divided by the yield normal force, F_Y , as a function of $1-\varepsilon$.



micromechanical model actually experimentally occurs for low loadings (below $\phi=0.10$).

For concentrations larger than $\phi=0.10$, the model underestimates the experimental data (c.f. Fig. 3). This is expected because of the presence of interaggregate interactions (Fernández-Toledano et al. 2014). Figure 3b demonstrates that the normal force is no longer proportional to the particle concentration and increases more rapidly (Ruiz-López et al. 2012). The slope is now closer to 3, in good qualitative agreement with observations by Guo et al. (2013). In their paper, see Fig. 6, they report a larger than 2 slope for the most concentrated suspensions. However, contrary to Guo et al. (2013), where magnetic field increased under compression, in our experimental assembly, the magnetic field distribution remains essentially constant during compression and this facilitates the interpretation of the results. The deviation from a slope of 2 for the most concentrated MR fluids will be later explained in terms of slip at the walls that favors interaggregate interactions when the aggregates come into contact (see below).

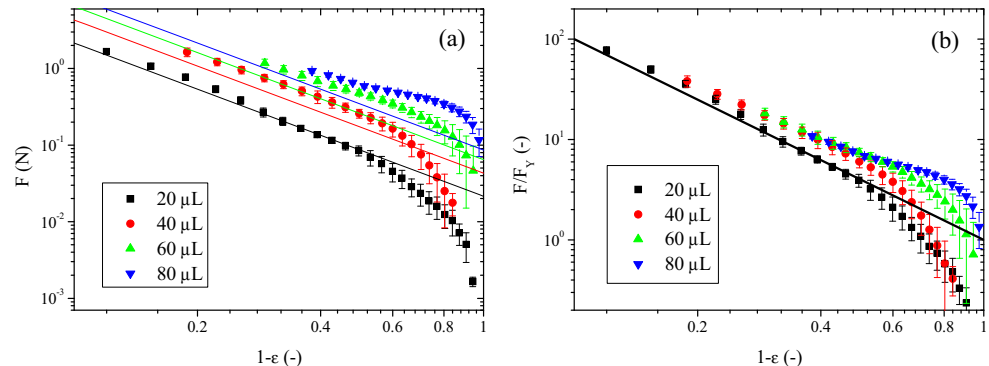
In the case of the lowest concentrations investigated (below $\phi=0.05$), the normal force sharply decreases for large $1-\varepsilon$ values, at the early stages of the deformation. Unfortunately, the normal force resolution of our magnetorheometer is approximately 0.01 N which is very close to the typical force corresponding to this drop, and therefore, we cannot get sound conclusions on this issue that, as stated above, may be related to inertia.

Effect of sample volume

As commented in the discussion of Fig. 3, the normal force resolution of the transducer impedes its accurate determination for large gap separations (large $1-\varepsilon$ values), especially for the lowest particle loadings where the sensed normal force is very small (below 1 N). In order to better explore this region, we decided to carry out further experiments involving larger sample volumes V_0 . These experiments would also be employed to test whether the theoretical prediction applies ($F \propto V_0$ according to Eq. 11).

Figure 4 contains experimental and theoretical predictions for initial volumes ranging from $V_0=20\ \mu\text{L}$ to $V_0=80\ \mu\text{L}$ in dilute MR fluids ($\phi=0.01$). As expected, larger $1-\varepsilon$ values (above the normal force resolution) can be reached because the resulting normal force increases. In qualitative agreement with the model, larger initial volumes give a larger normal force (c.f. Fig. 4a). However, only for the lowest initial volume explored ($V_0=20\ \mu\text{L}$), a good quantitative agreement is found between experiments and the theoretical prediction (i.e., a linear dependence is found). For the largest initial volumes, the model again underestimates the experimental data. These results are better appreciated in Fig. 4b. Figure 4b contains normalized normal force data for different sample volumes V_0 . For sufficiently small $1-\varepsilon$ values, experimental data collapse in very good quantitative agreement with the proposed theoretical model; a linear dependence is expected. However, for large V_0 , experimental data systematically

Fig. 4 Effect of sample volume, V_0 , on the compression behavior of dilute MR fluids ($\phi=0.01$). *Symbols*: experimental data. *Lines*: theoretical predictions (Eq. 11). Magnetic field strength $H_0=265\ \text{kA/m}$. Initial gap distance $h_0=300\ \mu\text{m}$. **a** Normal force, F , as a function of $1-\varepsilon$. **b** Normal force, F , divided by the yield normal force, F_Y , as a function of $1-\varepsilon$.



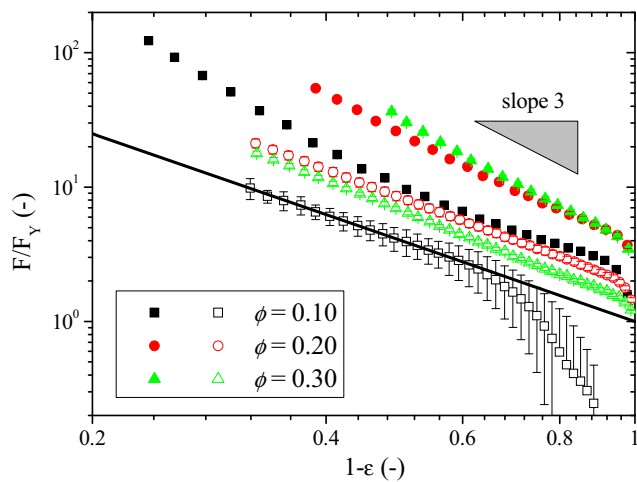


Fig. 5 Effect of plates surface roughness on the compression behavior of concentrated MR fluids ($\phi = 0.10, 0.20$, and 0.30 vol%). Smooth plates (closed symbols): $V_0 = 20 \mu\text{L}$; $h_0 = 300 \mu\text{m}$; $H_0 = 177 \text{ kA/m}$. Roughened plates (open symbols): $V_0 = 40 \mu\text{L}$; $h_0 = 600 \mu\text{m}$; $H_0 = 133 \text{ kA/m}$. Line: theoretical expression (Eq. 11)

deviate from the predictions, hence suggesting that inhomogeneities in the magnetic field distribution, which become more important for large V_0 and large $1 - \varepsilon$, influence the results.

Effect of surface roughness

According to the model (Eq. 11), a slope of 2 should be experimentally found when plotting the normalized force as a function of $1 - \varepsilon$ independently of the existence of slip or not. However, experiments reported for the larger concentrations explored ($\phi = 0.10, 0.20$, and 0.30) give a slope of nearly 3 (c.f. Fig. 3). To better understand these findings, we decided to carry out further experiments using roughened plates. In particular, the plates employed in these new experiments were subjected to sand-blasting and had a peak-to-valley roughness of $9.2 \mu\text{m}$.

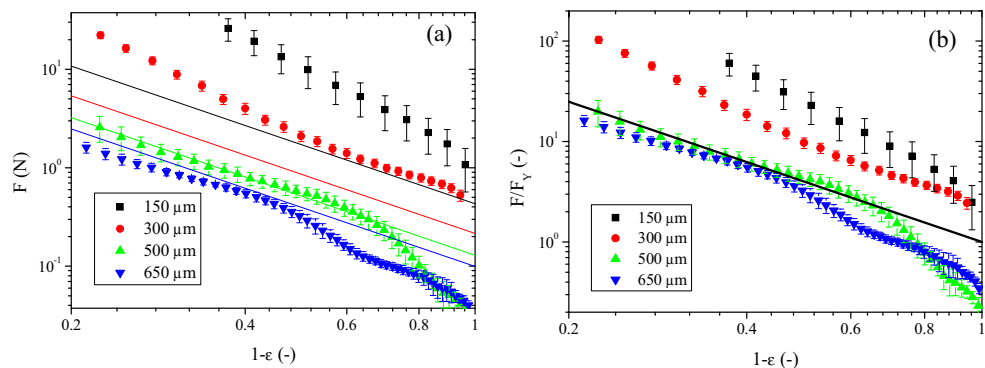
Results obtained for $\phi = 0.10, 0.20$, and 0.30 suspensions are contained in Fig. 5 and demonstrate that the slope is very close to 2 when rougher surfaces are used, in very good qualitative agreement with the model. This suggests that the

change in slope is actually mainly determined by slip of the MR fluid as a whole. Of course, the model still underestimates the experimental data because of the presence of interaggregate interactions at these particularly large particle loadings. In summary, the geometry assembly that is used by default in this work seems to prevent slip in the lowest concentrated MR fluids. However, for the largest concentrations investigated, the default roughness is not large enough to prevent slipping under this flow field. An important consequence of this is that the aggregates slipping along the surface can easily meet and form more complex interconnected structures therefore increasing the slope. By simply roughening the surfaces, slip is prevented and the slope becomes very close to 2 in agreement with the model. It is worth to note here that inhomogeneities in the field distribution do not explain the trends discussed in Fig. 5 because the wetted area is the same for all tests.

Effect of initial gap distance

According to the model described in the theoretical section, an initial gap distance, h_0 , dependence is expected. In particular, the magnetic contribution to the normal force scales with $F \propto h_0^{-1}$. Figure 6a demonstrates that the larger the gap distance the smaller the normal force, in good qualitative agreement with the model. This implies that the yield compressive stress decreases upon increasing the gap. The model is in a reasonably good agreement with the experiments for $h_0 > 300 \mu\text{m}$. However, for $h_0 \leq 300 \mu\text{m}$, the model underestimates the experimental normal force presumably because of the increasing importance of inhomogeneities in the magnetic field distribution in the magneto cell (note that V_0 is constant in this set of tests). Also, the hypothesis that magnetic particles self-assemble in straight single chains prior to the test is more difficult to achieve in view of the major importance of particle wall and interaggregate interactions at low h_0 values. In Fig. 6b, the normal force is scaled by the yield normal force F_Y . As shown, the initial gap scaling predicted by the model ($F \propto h_0^{-1}$) is in very good agreement with the experiments for $h_0 > 300 \mu\text{m}$.

Fig. 6 Effect of initial gap, h_0 , on the compression behavior of MR fluids. MR fluid concentration $\phi = 0.10$. Magnetic field strength $H_0 = 177 \text{ kA/m}$. Initial sample volume $V_0 = 20 \mu\text{L}$. **a** Normal force, F , as a function of $1 - \varepsilon$. **b** Normal force, F , divided by the yield normal force, F_Y , as a function of $1 - \varepsilon$.



Conclusions

A novel micromechanical model is proposed for the flow behavior of magnetorheological fluids in unidirectional slow compression. Even though this model is strictly valid in the dilute regime and for infinitesimally small deformations, it still explains experimental findings for a wide range of concentrations and deformations where the classical continuum media theory tends to fail (de Vicente et al. 2011b). In particular, the model provides an explanation for reported deviations from the slope of -2.5 that is theoretically predicted by continuous media theories. The predictions of the model are validated for different particle loadings, sample volume, surface roughness and gap distance.

Acknowledgments This work was supported by MAT 2013-44429-R and PCIN 2015-051 project (MINECO and FEDER) and by Junta de Andalucía P10-RNM-6630, P10-FQM-5977 and P11-FQM-7074 projects (Spain). J.A.R.-L. acknowledges financial support by the “Ministerio de Educación: Becas del Programa de Formación del Profesorado Universitario (FPU)” (AP2010-2144).

References

- Andablo-Reyes E, Hidalgo-Álvarez R, de Vicente J (2010) A method for the estimation of the film thickness and plate tilt angle in thin film misaligned plate-plate rheometry. *J Non-Newtonian Fluid Mech* 165:1419–1421
- Andablo-Reyes E, Hidalgo-Álvarez R, de Vicente J (2011) Erratum to “A method for the estimation of the film thickness and plate tilt angle in thin film misaligned plate-plate rheometry” *J. Non-Newtonian Fluid Mech*. 165 (2010) 1419–1421]. *J Non-Newtonian Fluid Mech* 166:882–882
- de Gans BJ, Hoekstra H, Mellema J (1999) Non-linear magnetorheological behaviour of an inverse ferrofluid. *Faraday Discuss* 112:209–224
- de Vicente J, López-López MT, Durán JDG, González-Caballero F (2004) Shear flow behavior of confined magnetorheological fluids at low magnetic field strengths. *Rheol Acta* 44:94–103
- de Vicente J, Klingenberg DJ, Hidalgo-Álvarez R (2011a) Magnetorheological fluids: a review. *Soft Matter* 7:3701–3710
- de Vicente J, Ruiz-López JA, Andablo-Reyes E, Segovia-Gutiérrez JP, Hidalgo-Álvarez R (2011b) Squeeze flow magnetorheology. *J Rheol* 55:753–779
- Engmann J, Servais C, Burbidge AS (2005) Squeeze flow theory and applications to rheometry: a review. *J Non-Newtonian Fluid Mech* 132:46388
- Ewoldt RH, Piotr T, McKinley G, Hosoi AE (2011) Controllable adhesion using field-activated fluids. *Phys. Fluids* 23(7): 073104
- Fernández-Toledano JC, Rodríguez-López J, Shahrivar K, Hidalgo-Álvarez R, Elvira L, Montero de Espinosa F, de Vicente J (2014) Two-step yielding in magnetorheology. *J Rheol* 58(5):1507–1534
- Guo CY, Gong XL, Xuan SH, Qin LJ, Yan QF (2013) Compression behaviors of magnetorheological fluids under nonuniform magnetic field. *Rheol Acta* 52(2):165–176
- Laun HM, Schmidt G, Gabriel C (2008) Reliable plate-plate MRF magnetorheometry based on validated radial magnetic flux density profile simulations. *Rheol Acta* 47:1049–1059
- Martin JE, Anderson RA (1996) Chain model of electrorheology. *J Chem Phys* 104(12):4814–4827
- McIntyre EC, Filisko FE (2010) Filtration in electrorheological suspensions related to the pecllet number. *J Rheol* 54(3):591–603
- Ruiz-López JA, Hidalgo-Álvarez R, de Vicente J (2012) On the validity of continuous media theory for plastic materials in magnetorheological fluids under slow compression. *Rheol Acta* 51(7):595–602
- Tang X, Zhang X, Tao R, Rong Y (2000) Structure-enhanced yield stress of magnetorheological fluids. *J Appl Phys* 87(5):2634–2638
- Volkova O, Bossis G, Guyot M, Bashtovoi V, Reks A (2000) Magnetorheology of magnetic holes compared to magnetic particles. *J Rheol* 44:91–104
- Xu Y, Gong X, Liu T, Xuan S (2014) Squeeze flow behaviors of magnetorheological elastomers under constant volume. *J Rheol* 58(3):659–679